Isolation and Purification of Active Antimicrobial Peptides from *Hermetia illucens* L., and Its Effects on CNE2 Cells

---- anticancer effect of antimicrobial peptides

Zhong Tian[#], Qun Feng[#], Hongxia Sun, Ye Liao, Lianfeng Du, Rui Yang, Xiaofei Li, Yufeng Yang, Qiang Xia[*]

Department of Immunology and Pathogenic Biology, Zhuhai Campus of Zunyi Medical University, Zhuhai 519041, P. R. China

[*]Corresponding author.

Tel: +86 13825633506; Fax: +86 7657623326

E-mail address: xiaqiang1973@126.com

[#]These two authors contributed equally to this work.

Summary Statement

1. An active antimicrobial peptide HI-3 was isolated and purified.
2. Inhibitory proliferation of CNE2 cells, but no effect on normal cells.
3. A potential antitumoral drug.

Abstract: Active antimicrobial peptide HI-3 was isolated and purified from the 5th instar larvae of *Hermetia illucens* L., and its effects on proliferation, apoptosis and migration of nasopharyngeal carcinoma (CNE2) cells were investigated. The expressions of telomerase reverse transcriptase (hTERT) in CNE2 cells were also studied *in vitro* to elucidate the mechanism involved in the action of HI-3 on CNE2 cells. Results showed that three fractions (HI-1, HI-2, HI-3) were isolated from the hemolymph of *H. illucens* larvae. After purified by RP-HPLC, only HI-3 showed the inhibitory activities to four strains of bacteria. It was also showed that HI-3 could effectively inhibit the proliferation of CNE2 cells in a dose- and time-dependent manner. Apoptosis of CNE2 cells was observed in the treatment with 160 μg/ml HI-3, and the early apoptosis rate up to 27.59 ± 1.14%. However, no significantly inhibitory effects and apoptosis were found on human umbilical vein endothelial cells (HUV-C). Moreover, HI-3 could significantly reduce the migration ability of CNE2 cells when compared with that of the control. On the other hand, the levels of mRNA and protein of hTERT in the HI-3 treatment were all significantly lower than that of the control. Results indicated that HI-3 could inhibit the proliferation of CNE2 cells and induce the apoptosis of CNE2 cells by down-regulating the telomerase activity in CNE2 cells, while no obvious effect was occurred on HUV-C. It inferred that HI-3 is a potential anti-tumor drug with low toxicity to normal cells.

Keywords: *Hermetia illucens*; proliferation; cell migration; apoptosis; telomerase

1. Introduction

More and more attentions were paid on the nasopharyngeal carcinoma (NPC) for its high incidence rates in Asia. Data from IARC showed that the incidence rates of NPC were up to 71.02% for men, which was nearly 2.45 times higher than that of women in Asian countries, especially in the country of Malaysia, Singapore, Indonesia and China (Mahdavifar et al., 2016). Currently, the traditional surgery combined with chemoradiotherapy was widely applied during its therapy. However, the radiotherapy and chemotherapy would inevitably damage the normal cells and the patient's immune systems (Ng and Lee, 2017), which more or less lead to the toxicity and severe effects in some tissues and organs (Thangavel et al., 2016). And the strong invasion ability of NPC cells and its inclination to distal metastasis made its treatments become more difficult (Jiang et al., 2014; Yang et al., 2013). Therefore, looking for a new, safe and effective anticancer agent for treatment of NPC has become a hot research direction worldwide.

Antimicrobial peptides (AMPs), the small molecule peptides that were firstly discovered by Boman research team, were found to have anti-bacterial, anti-viral, and anti-fungal properties. It was reported that AMPs could act rapidly to combat the invasion of potential pathogens, and thus serve to limit the extent of infection prior to activation of the adaptive immune response (Wanmakok et al., 2018). Furthermore, some of these peptides were found to display a wide range of biological activities and have been shown to exert antitumoral activity (Cerón et al., 2010). Nowadays, AMPs are considered as a potential alternative for the treatment of emerging drug-resistant infections and cancer (Riedl et al., 2011). The detailed mechanisms involved in antitumoral activities of AMPs were also

gradually established. Studies showed that AMPs might disrupt tumor cell membranes integrity and act on mitochondria or DNA to exert its antitumoral activity (Lemeshko, 2013). It was also reported that AMPs perform its anticancer effects by regulating the organisms' immune system. Studies have indicated that the organisms' immune defenses were enhanced by inducing dendritic cell aggregation and increasing the expression of lymphocytes after AMPs treatment, and the development of cancer was also inhibited (Huang et al., 2015).

In recent years, it was revealed that the telomerase might also be involved in the antitumoral mechanisms of AMPs. In normal cells, the expressions of telomerase were extremely low, or even none. However, their expression levels were significantly increased in malignant proliferative cells to protect their chromosomes and to promote the cells to proliferate indefinitely (Li et al., 2014; Ale-Agha et al., 2014). Generally, the main structure of telomerase includes telomerase reverse transcriptase (TERT) and telomerase-associated proteins (Blackburn et al., 2006). TERT, as the catalytic subunit of telomerase, plays a key role in telomerase synthesis and telomerase activity maintenance, especially in promoting the cells carcinogenesis (Borah et al., 2015). It was reported that higher levels of TERT mRNA were expressed in lung cancer–derived human cell line H1299, while lower levels in those of normal cells (Bodnar and Wright, 1998). Study also found that plasma TERT mRNA levels were significantly higher in the patients with liver cancer and prostate cancer than those in the normal group (El-Mazny et al., 2014), and the levels of TERT mRNA were closely related to various clinical and pathological conditions (Kang et al., 2013). Similar results were also reported by FU et al. (2015), which found that plasma hTERT mRNA levels in peripheral blood were significantly higher in patients with NPC than those in the

82 normal groups through the quantitative detection of telomerase hTERT mRNA. In addition,
83 the levels of telomerase hTERT mRNA were also been shown to be up-regulated, followed
84 by the G1/S blockade and chemotherapeutic drug resistance under hypoxia in NPC. Until
85 the hypoxia reversed, the telomerase activities were decreased, and chemo-resistance was
86 improved (Shi et al., 2015). From these studies, it was inferred that the telomerase activity
87 was closely related to the occurrence and development of NPC.

88 The black solider fly, *Hermetia illucens* L. is considered as a beneficial resource insect
89 in Diptera family. Its larvae are reported as feeding on immense variety of organic material,
90 and have been used in small-scale waste management purpose to reduce manure
91 accumulations in confined animal feeding operations and the accumulations of other wastes.
92 The habit of *H. illucens* larvae, which is extremely rich in various microorganisms including
93 many pathogenic ones, implies that the immune system of this insect functions works very
94 efficiently (Park et al., 2014). Since its first report in 2013 by our research group (Xia et al.,
95 2013), AMPs of this insect, which are essential components of innate immune system of *H.*
96 *illucens* larvae, have been paid more and more attentions and been considered to have
97 potential applications in the medicine fields (Choi and Jiang, 2014; Park et al., 2015; Vogel
98 et al., 2018). AMPs of *H. illucens* have showed good antibacterial activity for gram-positive
99 bacteria, gram-negative bacteria and fungi (Elhag et al., 2017). However, no research was
100 focused on their anti-cancer activity and related mechanisms. Therefore, in the present study,
101 the AMPs were isolated and purified from the hemolymph of *H. illucens* larvae, and the
102 active components HI-3 were screened out to investigate its effects on the proliferation,
103 apoptosis and migration of nasopharyngeal carcinoma (CNE2) cells. Furthermore, the

104 expressions of telomerase in CNE2 cells were also studied to explore the possible
105 mechanism of HI-3 action. We hope the results would provide theoretical basis for the
106 research and development of the *H. illucens* AMPs as a potential antitumoral agent.

107

108 **2 Materials and methods**

109 **2.1 Insects, bacteria and cells**

110 *H. illucens* L. was provided by Zhuhai Modern Agriculture Development Center. The
111 larvae were feed with artificial feed (wheat bran: corn flour: chick feed=5: 3: 2) and kept in a
112 greenhouse of 27 □, RH 80%, photoperiod 14 L: 10 D.

113 The four strains of bacteria *Staphylococcus aureus*, *Escherichia coli*, *Bacillus subtilis*, and
114 *Enterobacter aerogenes* were obtained from Immunology and Pathogenic Biology Laboratory
115 of Zunyi Medical University.

116 Standard strains of human CNE2 cells and human umbilical vein endothelial cells
117 (HUV-C) were purchased from Shanghai ATCC Cell Bank of Chinese Academy of Sciences.

118 Tricine-SDS PAGE gel kit was purchased from Sigma; CCK-8 kit, Hoechst33342 staining
119 kit, and Annexin V-FITC/PI double staining kit were purchased from Japan Tongren Institute
120 of Chemistry; RT-PCR telomerase detection kit was purchased from Nanjing Kaiji Biological
121 Co., Ltd.; hTERT antibody was purchased from ABclonal Company.

122 Vertical electrophoresis (Mini-PROTEAN Tetra), Horizontal electrophoresis(YCP-31DN),
123 Automatic microplate reader(Elx-800), RT-PCR (621BR07707) were from Bio-Rad;
124 RP-HPLC (LC-C8002) was from Shimadzu Corporation; Inverted fluorescence microscopy
125 (IX71) was from OLYMPUS Corporation; Flow cytometry (FACS Calibur) was from
126 Beckman Coulter Corporation.

127

2.2 Induction and Extraction AMPs from the larvae of *H. illucens*

According to the method mentioned in Xia et al (2013), the 20,000 fifth instar larvae of *H. illucens* were selected for induction. The larvae in the induction group were received abdomen acupuncture treated with *Staphylococcus aureus* (A260=2.4), while those in the control group were acupunctured with culture medium. After 24 h treatment, the hemolymph of larvae in the induction and control group was collected into Eppendorf centrifuge tubes and centrifuged at 12,000 rpm for 10 min at 4°C. Then, the supernatant was transferred into a 10 kD ultrafiltration centrifuge tube and centrifuged at 12,000 rpm for 15 min at 4 °C. The ultrafiltrate was again transferred to a 3 kD ultrafiltration centrifuge tube and centrifuged under the same conditions. The retention section, which is AMP crude extract, was freeze-dried in vacuo and stored in a refrigerator at -80 □ for use.

2.3 Purification of AMPs from crude extract

The crude extract of AMPs was separated by RP-HPLC system. The column was the type of LC-C8002, 4.6 mm × 250 mm, 10 μm, and column temperature at 40 □. The mobile phase was 0.1% (v/v) TFA (phase A) and acetonitrile with 0.1% TFA (phase B) at a flow rate of 0.5 ml/min. UV detector wavelength was set at 214 nm. According to the retention time of the peak, the components corresponding to each peak were collected.

Purity of HI-3 was also detected by RP-HPLC. And the chromatographic conditions were same as mentioned above 0.5 ml/min, detection wavelength 214 nm, temperature 40 □.

2.4 Antibacterial activity assays

Four strains of bacteria, *Staphylococcus aureus*, *Escherichia coli*, *Bacillus subtilis* and *Enterobacter aerogenes*, were formulated into bacterial liquid at the concentration of 3.2

152 $\times 10^{12}$/ml, separately. Then, 50 μl of each bacterial liquid was evenly coated in the LB solid
153 medium. When the bacterial liquid was dry, the sterile filter paper with a diameter of 6mm,
154 which were treated with 25 μl of Gentamicin sulfate (as positive control), saline (as negative
155 control) and purified AMPs (named as HI-1、HI-2、HI-3) separately, were placed on the
156 medium. Four replicates were set. After incubated at 37 °C for 24 h, the size of the inhibition
157 zone was observed and measured (Xia et al., 2013).

158 The value of MIC (minimum inhibitory concentration) about the component HI-3 with
159 strong antibacterial activity was detected by MH broth dilution method. Gentamicin sulfate
160 was used as positive control. Absorbance value was read at 595 nm to calculate the inhibition
161 rate Y.

162 $Y = (A0 - A1) / (A0 - A2) \times 100\%$

163 Among them，A0 is the absorbance value in the negative control, A1 is the value in the HI-3
164 treatment, and A2 is the value in positive control.

165 MIC was recorded as the minimum inhibitory concentration at which the inhibition rate
166 was not less than 80%.

167

168 **2.5 Estimation of cytotoxicity in CNE2 cells and HUV-C**

169 To test the cell viability after treatment with HI-1, HI-2 and HI-3, CCK-8 kit was run.
170 Cells were plated at a density of $1x10^5$ cells/100 μl/well in 96-well plates for 24 h. Four
171 replicates were set for each treatment. Then, the medium was discarded and replaced by
172 different concentrations (5 μl/ml, 10 μg/ml, 20 μg/ml and 40 μg/ml) of HI-1, HI-2, HI-3,
173 respectively, or medium alone for 24 h and 48 h. This was followed by the addition of 20 μl
174 of CCK-8 solution for 2 h at 37 °C in 5% CO_2 incubator. The optical density was measured
175 spectrophotometrically at 490 nm on a microtiter plate reader. Results were expressed as a

176 percentage of the inhibition rate for viable cells, and values of the medium only group were
177 regarded as negative control.

178 Inhibition rate (%) = $(A_{\text{negative control}}-A_{\text{treatment}})/A_{\text{negative control}}$

179

180 **2.6 Effects of HI-3 on apoptosis and migration of CNE2 cells**

181 **2.6.1 Apoptosis of CNE2 cells**

182 The CNE2 cells and HUV-C were maintained in RPMI-1640 and DMEM medium
183 supplemented with 10% FBS, respectively. Cells were maintained in incubator under a fully
184 humidified atmosphere of 95% room air and 5% CO_2 at 37 □. Briefly, the cell density was
185 adjusted to 1×10^5 cells/ml, and 100 μl of cell suspensions were placed onto 96-well plates.
186 Four replicates were set for each treatment. The medium was removed after 24 h, and HI-3
187 was added to cell cultures at a final concentration of 40 μg/ml, 80 μg/ml and 160 μg/ml. After
188 incubation for 48 h at 37 □ in a humidified atmosphere with 5% CO_2, 5 μl of Hoechst33342,
189 a DNA specific fluorescent dye, which stains the condensed chromatin of apoptotic cells more
190 brightly than the chromatin of normal cells, was added to each well and incubated for 15
191 minutes at room temperature. Morphological changes in nuclear chromations of cells in
192 control and each treatment were observed with fluorescence microscope, and the influence of
193 HI-3 on the apoptosis rate of CNE2 cells and HUV-C was detected by flow cytometry (FCM)
194 (Yan et al., 2015).

195

196 **2.6.2 Migration of CNE2 Cells**

197 The HUV-C and CNE2 cells suspension was prepared as the method mentioned in 2.7.1.
198 2 ml of cell suspension was placed into a 6-well plate and incubated at 37 °C in the incubator
199 with 5% CO_2. After the cells were fully covered the plate, the cells in each well was

perpendicularly streaked with a 200 μl of pipette tip, followed by washing with PBS. Then, 2 ml of HI-3 diluted with 2% FBS and 0.2% colchicine was added to cell cultures at a final concentration of 160 μg/ml, while the negative control received with the same volume of solution without HI-3. After 0 h, 12 h, 24 h and 48 h incubation, the scratches were observed and photographed to calculate the mobility.

Mobility (%) = (W0-WK)/W0 × 100%

Among them, W0 is the width of scratches at 0 h, WK is the width of scratches at 12 h, 24 h, 48 h, respectively.

2.7 RT-PCR analysis of telomerase hTERT gene expression

RT-PCR was used to analyze gene expression of telomerase hTERT in CNE2 cells treated with 160 μg/ml of HI-3 for 48 h. And the cells without treatment were set as control. The primers used for hTERT were upstream 5'-GCCGATTGTGAACATGGACTACG-3' and downstream 5'-GCTCGTAGTTGAGCACGCTGAA-3'. Primer pair for GAPDH (upstream 5'-CATCTTCTTTGCGTCGCCA-3'; downstream '5-TTAAAAGCAGCCCTGGTGACC-3') was used as the reference gene. Reaction system involved each 1 μl of primers of upstream and downstream, 2 μl of template RNA, 2.75 μl of RT-PCR MIX (including reverse transcriptase, Taq DNA polymerase and RNase inhibitor), 25 μl of 2× reaction buffer, and RNase free water which was added to a total volume of 50 μl. The samples were denatured at 94 °C for 5 min, followed by a 40 cycles reaction: 94 °C for 30 s, 60 °C for 30 s, 72 °C for 1 min; and by the extension at 72 °C for 10 min. The 10 μl of PCR products were separated by 1% agarose gel electrophoresis, and the expressions of hTERT gene were analyzed by $2^{-\Delta\Delta Ct}$ method using GAPDH as internal reference gene.

2.8 Western blotting analysis of the telomerase hTERT protein expression

Western blotting for detecting telomerase hTERT was performed after CNE2 cells were treated with HI-3 at the final concentration of 160 μg/ml for 48 h. Briefly, the cells were harvested and the cellular protein were extracted by homogenization in 100 μl lysate on ice for 30 min. The lysates were then centrifuged at 12,000 rpm for 30 min at 4 □. The proteins were quantified using the Bradford method, and 30 μg proteins were separated using SDS-PAGE gel and transferred onto PVDF membranes (Millipore, USA). Non-specific binding was prevented using a solution of 5% non-fat dry milk at room temperature for 1 h, and then washed with TBST for 3 times. Blots were incubated with the primary antibody diluted 1: 1000 primary antibody (for hTERT and GAPDH) diluted with 2% BSA in TBS containing 0.1% Tween-20 (TBST) overnight at 4 °C. After washing with TBST for 3 times, the blots were incubated with mouse-derived secondary antibody diluted 1: 3000 with 1% BSA in TBST for 1 h at room temperature. Following additional washing, gray-scale of specific bands was detected with ECL development.

2.9 Statistical analysis

Results were expressed as means ± SEM. To analyze the differences between control and treatments, single-factor analysis of variance in SPSS 20.0 software was used. Statistical differences were considered significant at a value of $P < 0.05$.

3 Results

3.1 Isolation and purification of antimicrobial peptides

The crude extract from the hemolymph of *H. illucens* larvae is clear and transparent, and exhibits white powder after freeze-dried in vacuo. After PR-HPLC analysis, three compounds, HI-1, HI-2 and HI-3, were well separated from the crude extract in the induced group (Figure 1-1)). And the purity of HI-3 was up to 96.1% after purification (Figure 1-2)).

3.2 Antibacterial activity of three separated components

As shown in Table 1, only HI-3 showed significant antibacterial activity on the all four strains of bacteria when compared with that in the negative control ($P < 0.05$). Furthermore, the antibacterial activity of HI-3 to *Bacillus subtilis* (10.84 ± 1.00 mm) *Staphylococcus aureus* and *Escherichia coli*, which inhibition zone diameter was 10.84 ± 1.00 mm, was significantly lower than that to *Staphylococcus aureus* (11.79 ± 1.178 mm), *Escherichia coli* (11.83 ± 0.82 mm) and *Enterobacter aerogenes* (11.41 ± 0.78 mm) ($P < 0.05$).

3.3 MIC of HI-3 to the four strains of bacteria

From Figure 2, it was indicated that inhibitory rates of HI-3 against the four types of bacteria were all positively correlated with the concentration of active component HI-3. After analysis, the MICs of HI-3 to *Staphylococcus aureus, Bacillus subtilis, Escherichia coli* and *Enterobacter aerogenes* were 80 μg/ml, 160 μg/ml, 80 μg/ml and 80 μg/ml, respectively. From these results, it can be seen that the HI-3 was less sensitive to *Bacillus subtilis* than those of the other three bacteria, which was similar to the results of antibacterial activity of HI-3.

3.4 HI-3 induces cytotoxicity on CNE2 cells

According to the growth curve of CNE2 cells and HUV-C detected by CCK-8 kit, CNE2 cells entered logarithmic growth phase on the 2nd day, while HUV-C on the 3rd day. Therefore, CNE2 cells after 2 days of culture and HUV-C after 3 days of culture were chosen for follow-up experiments, respectively, to verify the effects of HI-1, HI-2 and HI-3 on the proliferation of the two cells.

The dose- and time-dependent effects of HI-1, HI-2 and HI-3 against CNE2 cells were shown in Table 2. No significant effects on the proliferation of CNE2 cells were found after treatment with HI-1 and HI-2 for 12 h, 24 h and 48 h, respectively. When the concentration of HI-3 was among 40-160 μg/ml, HI-3 exhibited significantly inhibitory activity on the proliferation of CNE2 cells when compared to that in the corresponding HI-1 and HI-2 groups ($P < 0.05$). Furthermore, the inhibitory rate on the proliferation of CNE2 cells also increased with the treatment period of HI-3 at the concentration of 40-160 μg/ml, and the maximal inhibitory rate was recorded in the 160 μg/ml HI-3 after 48 h treatment (Table 2; Figure 3). By contrast, HI-3 treatment had no significant effect on the proliferation of HUV-C ($P > 0.05$) (Data not shown).

3.5 HI-3 induced apoptosis of CNE2 cells

To investigate the mode of action underlying the cytotoxic activity of HI-3 at the concentrations of 40-160 μg/ml, the CNE2 cells and HUV-C were incubated with HI-3 for 48 h for fluorescence microscope and FCM.

Representive micrographs by fluorescence microscope revealed that the CNE2 cells in the control was membrane-intact and light blue, and the emitted fluorescence was weak (Figure 4-1)-A). After 48 h treatment with 40 μg/ml HI-3, increased fluorescence intensity was observed in the CNE2 cells, indicating that HI-3 disrupted the integrity of the plasma membrane, and the symptoms of early apoptosis occurred. However, the fluorescence intensity is still uniform, which meant that the chromosomal DNA was not destroyed. With the increasing HI-3 concentration, the fluorescence intensity in CNE2 cells was further improved, indicating that the permeability of the plasma membrane was gradually increased (Figure 4-1)-B, 4-1)-C). When the concentration of HI-3 was up to 160 μg/ml, the CNE2 cells exhibited the strongest fluorescence intensity, and the number of brightly stained cells with DNA damage was also increased. Furthermore, the typical characteristics of cell apoptosis,

300 such as highly aggregated and fragmented chromatin, and dispersed apoptotic bodies, were
301 appeared. These results exhibited that high concentration of HI-3 induced drastic changes in
302 the cellular morphology (Figure 4-1)-D, arrow).

303 By contrast, there were no obvious changes in the morphology of HUV-C after treated with
304 different concentrations of HI-3 for 48 h (Figure 4-2)).

305 Results from FCM detection showed that exposure to HI-3 at the concentrations of 40-160
306 μg/ml for 48h caused a dose-dependent increase in the apoptosis rate of CNE2 cells compared
307 to that of the control cells. And the apoptosis rate in all the treatments was all significantly
308 higher than that in the control ($P < 0.05$), as well as higher than that in the corresponding
309 HUV-C. The results demonstrated that HI-3 induced apoptosis of CNE2 cells after 48 h
310 exposure (Figure 5-1); 5-3)). Same to the fluorescence microscope results, HI-3 exposure did
311 not resulted in significantly improved apoptosis rate in the HUV-C (Figure 5-2); 5-3)).

312

313 **3.6 HI-3 inhibited the Migration of CNE2 cells**

314 After making a wound with a pipette tip, it was observed that HI-3 effectively inhibited the
315 migration of CNE2 cells in time-dependent manners when compared to the untreated control
316 cells. The migration rate of CNE2 cells exposed to 160 μg/ml HI-3, which was 24.43 ± 0.47%,
317 61.5 ± 0.04% and 80 ± 0.33%, respectively, were all significantly lower than that of cells in
318 the control (50.3 2± 0.24%, 91.17 ± 0.15% and 100%) ($P < 0.05$) (Figure 6).

319

320 **3.7 Effect of HI-3 on telomerase hTERT gene expression in CNE2 cells**

321 As showed in Figure 14, the brightness of 28S band is about 2 times of that of 18S band,
322 and no tailing phenomenon occurred, indicating that the RNA quality is qualified without
323 degradation and DNA contamination. After HI-3 treatment for 48 h, the expression of hTERT

mRNA was significantly down-regulated in the CNE2 cells compared with that in the control ($P < 0.05$) (Figure 7-1); Table 3). Simultaneously, telomerase hTERT protein expression also significantly decreased. The expression of hTERT protein in the control cells (1.19 ± 0.21) was significantly higher than that in the HI-3 treated cells (0.63 ± 0.12) by gray value analysis ($P < 0.05$) (Figure 7-2), 7-3)).

4 Discussion

In this study, we demonstrated that a small molecule peptide HI-3, purified from the hemolymph of *H. illucens* larvae after acupuncture induction with *Staphylococcus aureus*, showed inhibitory effects on both gram-positive and gram-negative bacteria, as well as on the proliferation of CNE2 cells to some extent. It was also found that HI-3 could induce the apoptosis and inhibit the migration of CNE2 cells. Further studies confirmed that HI-3 could significantly inhibit the expression of hTERT. An interesting observation in this study is that HI-3 had more deleterious effects towards CNE2 cells than toward normal cells. Its antitumor activity towards CNE2 cells was unlike that of chemotherapeutic agents, for they cannot discriminate between normal and cancer cells. These results support our assumption that HI-3 may act on a potential antitumor drug without toxic development.

After acupuncture induction with *Staphylococcus aureus*, three components were separated from the hemolymph of *H. illucens* larvae. However, only HI-3 showed different degrees of antibacterial activities against all selected bacteria, which was consistent with the broad-spectrum antibacterial effects of AMPs reported in the previous studies. Generally, AMPs exert their antibacterial activity through the destruction of the plasma membrane (Lee et al., 2015a; Nguyen et al., 2011). Due to their amphipathic nature, most of AMPs are positively charged and can interact with the negatively charged phospholipid bilayer on the bacterial surface by electrostatic action or with other anions on the membrane to form ion channels on the plasma membrane (Huang et al., 2010). It was found that the AMP attacins

from the silkworm could inhibit the growth of gram-negative bacteria by inhibiting the synthesis of membrane proteins; and moricin, another antibacterial peptide, could exert its antimicrobial activity by increasing membrane permeability (Ravi et al., 2011). Though the plasma membranes of CNE2 cells were disrupted by HI-3 treatment in this study, whether the mechanism of HI-3 against bacteria was through this action still need further study.

AMPs isolated from insects, including melittin, cecropin related peptides and magainins have been shown to exhibit antitumoral activity for cells derived from mammalian tumors (Lee et al., 2015b; Su et al., 2015). In the present study, HI-3 at the concentration of 40-160 μg/ml also exhibited the proliferation inhibition of CNE2 cells in a dose- and time- dependent manner. However, the negative control cells HUV-C were not affected by HI-3 treatment. These results were similar to the study of Wang et al. (2012), which found that the AMP temporin-1CEa have different degrees of inhibition against the growth of various types of tumor cells, while normal human erythrocytes and HUVSMCs cells were not affected. Different studies have attempted to explain the mechanisms that the tumor cells are more sensitive to AMPs treatments (Wang et al., 2016). For the surface of tumor cells membrane holds more negatively charged phosphatidylserine, abnormal expressed polysaccharide proteins and increased sialylation when compared with the normal cells, some investigations have determined that one of its antitumoral mechanisms was through destructing the cell membrane, which was similar to that of the antibacterial activity. For example, Slaninová et al. (2012) demonstrated that AMP from wild-type bee venom exerted the cytotoxic effects on tumor cells through enhancing the permeability of tumor cell membranes. Chang et al. (2011) reported that the AMP tilapia hepcidin(TH)1-5 could bind to the membranes of HepG2 and HeLa tumor cells, breaking the cell membrane through a process similar to that of cytolysis, and eventually lead to cell necrosis. In addition, the toxicity of AMP D-peptide from beetles against tumor cells mainly depended on the negative charge carried by phosphatidylserine in the tumor cell membrane (Iwasaki et al., 2009). In present study, fluorescence intensity in CNE2 cells increased with the increasing concentration of HI-3 in a dose-dependent manner,

indicating that the target site of HI-3 might also be the membrane. Furthermore, the increasing apoptosis rates in CNE2 cells after HI-3 treatment might also be related with the gradually improved membrane permeability, though more researches should be investigated.

HI-3 was able to inhibit the migration of CNE2 cells to a certain extent according to our cell scratch assay. Generally, tumor cells have a strong ability of invasion and metastasis. Distal metastasis and subsequent increased malignant proliferative capacity are among the major problems during the oncotherapy. Relevant study revealed that an amphibian AMP Temporin-1CEa could inhibit the invasion and metastasis of melanoma A375 cells whereby regulating the release of metalloproteinase-2 and vascular growth factor (Zhang, 2015). However, few studies have focused on the specific mechanisms concerning the migration of cancer cells treated with AMP. The deep research remains to be explored.

Higher activity telomerase could be detected in malignant proliferative cancer cells. Therefore, telomerase is considered as an important and effective target for anti-tumor therapy (Chen et al., 2016). For example, the growth inhibition of human colon cancer HCT166 cells by AZT (3'-Azido-3'-deoxythymidine) was mediated by inhibiting telomerase activity and hTERT gene expression (Hu and Xu, 2017). Our study also found that hTERT gene expression and hTERT protein expression were significantly decreased after HI-3 treatment, indicating that the down-regulating of telomerase activity was involved in the inhibition of NPC. On the other hand, it was reported that in addition to its function of maintaining intracellular DNA and chromosomes stability, telomerase is also involved in the regulation of mitochondrial function and gene expression during tumorigenesis (Chiodi and Mondell, 2012). For hTERT is the key protein of telomerase synthesis, it might also be involved in the action of telomerase in the occurrence and development of cancer. However, the regulation effect of telomerase and hTERT in the HI-3 induced inhibition of proliferation of CNE2 cells still need further investigation. And whether the mitochondrial pathway was induced in the HI-3 action also remains to be explored.

403 From these results, we concluded that HI-3 has the potential for development as a new
404 type of antitumoral agent, for HI-3 is less toxic to normal cells. It was confirmed that HI-3
405 might exert its antitumoral effect through down-regulating the expression of hTERT.
406 However, the specific mechanism involved in the HI-3 still need deep investigations.

Acknowledgements

We thank Prof. Guren Zhang for comments that greatly improved the manuscript, and we thank the “anonymous” reviewers for their constructive suggestions.

Competing interests

The authors have declared that no competing interests exist.

412 **Author contributions**

413 Zhong Tian and Qun Feng performed the experiments, Hongxia Sun and Ye Liao drafted
414 and revised the manuscript, Lianfeng Du and Rui Yang performed the data analyses, Xiaofei
415 Li and Yufeng Yang helped perform the analysis with constructive discussions, and Qiang
416 Xia designed the experiments.

Funding

This work was supported by the grants from The Major Research Project of the Innovation Group of the Education Department of Guizhou Province (KY characters [2016]037 in Guizhou Province); The National Nature Sciences Fund (31260528); and Guizhou Science and Technology Fund (KY characters [2009]2295 in Guizhou Province).

References

Ale-Agha, N., Dyballa-Rukes, N., Jakob, S., Altschmied, J., and J. Haendeler. (2014). Cellular functions of the dual-targeted catalytic subunit of telomerase, telomerase reverse transcriptase --potential role in senescence and aging. *Exp Gerontol*. 56, 189-193.

Blackburn, E. H., Greider, C. W., and J. W. Szostak. (2006). Telomeres and telomerase: the path from maize, Tetrahymena and yeast to human cancer and aging. *Nat Med*. 12, 1133-1138.

Bodnar, A. G., and Wright, W. E. (1998). Extension of life-span by introduction of telomerase into normal human cells. *Science*. 279, 349-352.

Borah, S., Xi, L., Zaug, A. J., Powell, N. M., Dancik, G. M., Cohen, S. B., Costello, J. C., Theodorescu, D., and Cech, T. R. (2015). Cancer. TERT promoter mutations and telomerase reactivation in urothelial cancer. *Science*. 347, 1006-1010.

Cerón, J. M., Contreras, M. J. E., de Cienfuegos, G. A., Puertollano, M. A., andde Pablo, M. A. (2010). The antimicrobial peptide cecropin A induces caspase-independent cell death in human promyelocytic leukemia cells. *Peptides*. 31, 1494-1503

Chang, W. T., Pan, C. Y., Rajanbabu, V., Cheng, C. W., and Chen, J. Y. (2011). Tilapia (*Oreochromis mossambicus*) antimicrobial peptide, hepcidin 1-5, shows antitumor activity in cancer cells. *Peptides*. 32, 342-352.

Chen, Y. Y., Wu, X. Q., Tang, W. J., Shi, J. B., Li, J., and Liu, X. H. (2016). Novel dihydropyrazole-chromen: design and modulates hTERT inhibition proliferation of MGC-803. *Eur J Med Chem*. 110, 65-75.

Chiodi, I., and Mondello, C. (2012). Telomere-independent functions of telomerase in nuclei, cytoplasm, and mitochondria. *Front Oncol*. 2, 133-139.

445 Choi, W. H., and Jiang, M. H. (2014). Evaluation of antibacterial activity of hexanedioic acid
446 isolated from *Hermetia illucens* larvae. *J Appl. Biomed*. 12, 179-189.

447 Elhag, O., Zhou, D., Song, Q., Soomro, A. A., Cai, M., Zheng, L., Yu, Z., and Zhang, J.
448 (2017). Screening, expression, purification and functional characterization of Novel
449 Antimicrobial Peptide Genes from *Hermetia illucens* (L.). *PloS One*. 12, e0169582.

450 El-Mazny, A., Sayed, M., and Sharaf, S. (2014). Human telomerase reverse transcriptase
451 messenger RNA (TERT mRNA) as a tumor marker for early detection of hepatocellular
452 carcinoma. *Arab J Gastroenterol*. 15, 68-71.

453 Fu, X. S., Shen, C. X., Li, G. X., Zhang, X. Y., and Wen, Z. (2015). Quantitative detection of
454 plasma level of human telomerase reverse transcriptase mRNA in patients with
455 nasopharyngeal carcinoma. *J South Med Univ*. 35, 894-897.

456 Hu, T. H., and Xu, X. X. (2017). Effects of telomerase inhibitors on proliferation and
457 apoptosis of human colon cancer HCT116 cells in different aneuploidy states. *Chin J Cell*
458 *Biol*. 39, 426-434.

459 Huang, H. N., Rajanbabu, V., Pan, C. Y., Chan, Y. L., Chen, J. Y., and Wu, C. J. (2015).
460 Enhanced control of bladder-associated tumors using shrimp anti-lipopolysaccharide factor
461 (SALF) antimicrobial peptide as a cancer vaccine adjuvant in Mice. *Mar Drugs*. 13,
462 3241-3258.

463 Huang, Y., Huang, J., and Chen, Y. (2010). Alpha - helical cationic antimicrobial peptides:
464 relationships of structure and function. *Protein Cell*. 1, 143-152.

465 Iwasaki, T., Ishibashi, J., Tanaka, H., Sato, M., Asaoka, A., Taylor, D., and Yamakawa, M.
466 (2009). Selective cancer cell cytotoxicity of enantiomeric 9-mer peptides derived from beetle
467 defensins depends on negatively charged phosphatidylserine on the cell surface. *Peptides*. 30,
468 660-668.

469 Jiang, H. G., Gao, M., Shen, Z., Luo, B., Li, R., Jiang, X., Ding, R., Ha, Y., Wang, Z., and Jie,
470 W. (2014). Blocking PI3K/Akt signaling attenuates metastasis of nasopharyngeal carcinoma
471 cells through induction of mesenchymal-epithelial reverting transition. *Oncol Rep*, 2014, 32:
472 559-566.

473 Kang, Y., Zhang, J., Sun, P., Shang, J. (2013). Circulating cell-free human telomerase reverse
474 transcriptase mRNA in plasma and its potential diagnostic and prognostic value for gastric
475 cancer. *Int J Clin Oncol*. 18, 478-486.

476 Lee, H., Hwang, J. S., Lee, J., Kim, J. I., and Lee, D. G. (2015a). Scolopendin 2, a cationic
477 antimicrobial peptide from centipede, and its membrane-active mechanism. *Biochim Biophys*
478 *Acta*. 1848, 634-642.

479 Lee, J. H., Kim, I., Kim, S., Yun, E., Nam, S., Ahn, M., Kang, D., and Hwang, J. S. (2015b).
480 Anticancer activity of CopA3 dimer peptide in human gastric cancer cells. *BMB Rep*. 48,
481 324-329

482 Lemeshko, V. V. (2013). Electrical potentiation of the membrane permeabilization by new
483 peptides with anticancer properties. *Biochim Biophys Acta*. 1828, 1047-1056.

484 Li, P., Tong, Y., Yang, H., Zhou, S., Xiong, F., Huo, T., and Mao, M. (2014). Mitochondrial
485 translocation of human telomerase reverse transcriptase in cord blood mononuclear cells of
486 newborns with gestational diabetes mellitus mothers. *Diabetes Res Clin Pract*. 103, 310-318.

487 Mahdavifar, N., Ghoncheh, M., Mohammadian-Hafshejani, A., Khosravi, B., and Salehiniya,
488 H. (2016). Epidemiology and inequality in the incidence and mortality of nasopharynx cancer
489 in Asia. *Osong Public Health Res Perspect*. 7, 360-372.

490 Ng, J., and Lee, P. (2017). The Role of Radiotherapy in Localized Esophageal and Gastric
491 Cancer. *Hematol Oncol Clin North Am*. 1, 245-257.

492 Nguyen, L. T., Haney, E. F., and Vogel, H. J. (2011). The expanding scope of antimicrobial
493 peptide structures and their modes of action. *Trends Biotechnol*. 29, 464-472.

494 Park, S., Chang, B. S., and Yoe, S. M. (2014). Detection of antimicrobial substances from
495 larvae of the black soldier fly, *Hermetia illucens* (Diptera: Stratiomyidae). *Entomol Res*. 44,
496 58-64.

497 Park, S. I., Kim, J. W., and Yoe, S. M. (2015). Purification and characterization of a novel
498 antibacterial peptide from black soldier fly (*Hermetia illucens*) larvae. *Dev Comp Immunol*.
499 52, 98-106.

500 Ravi, C., Jeyashree, A., and Renuka Devi, K. (2011). Antimicrobial peptides from insect: An
501 overview. *Res in Biotech*. 2, 1-7.

502 Riedl, S., Zweytick, D., and Lohner, K. (2011). Membrane-active host defense
503 peptides-challenges and perspectives for the development of novel anticancer drugs. *Chem*
504 *Phys Lipids*. 164, 766-781.

505 Shi, X., Liu, Y. H., Shen, C. X., Wen, Z., Li, G. X., and Fu, X. S. (2015). Up-regulated
506 telomerase and inhibited proliferation induced by hypoxia in nasopharyngeal carcinoma cells.
507 *Chin J Cancer Prev Trea*. 22, 507-513.

508 Slaninová, J., Mlsová, V., Kroupová, H., Alán, L., Tůmová, T., Borovičková, L., Fučík, V.,
509 and Ceřovský, V. (2012). Toxicity study of antimicrobial peptides from wild bee venom and
510 their analogs toward mammalian normal and cancer cells. *Peptides*. 33, 18-26.

511 Su, M., Chang, W., Cui, M., Lin, Y., Wu, S., and Xu, T. (2015). Expression and anticancer
512 activity analysis of recombinant human uPA1□43-melittin. *Int J Oncol*. 46, 619-626.

513 Thangavel, S., Yoshitomi, T., Sakharkar, M. K., and Nagasaki, Y. (2016). Redox nanoparticle
514 increases the chemotherapeutic efficiency of pioglitazone and suppresses its toxic side effects.
515 *Biomaterials*. 99, 109-123.

516 Vogel, H., Müller, A., Heckel, D. G., and Vilcinskas, A. (2018). Nutritional immunology:
517 Diversification and diet-dependent expression of antimicrobial peptides in the black soldier
518 fly *Hermetia illucens*. *Dev Comp Immunol*. 78, 141-148.

519 Wang, C., Chen, Y. W., Zhang, L., Gong, X. G., Zhou, Y., and Shang, D. J. (2016).
520 Melanoma cell surface-expressed phosphatidylserine as a therapeutic target for cationic
521 anticancer peptide, temporin-1CEa. *J Drug Target*. 24, 548-556.

522 Wang, C., Li, H. B., Li, S., Tian, L. L., and Shang, D. J. (2012). Antitumor effects and cell
523 selectivity of temporin-1CEa, an antimicrobial peptide from the skin secretions of the Chinese
524 brown frog (*Rana chensinensis*). *Biochimie*. 94, 434-441.

525 Wanmakok, M., Orrapin, S., Intorasoot, A., and Intorasoot, S. (2018). Expression in
526 *Escherichia coli* of novel recombinant hybrid antimicrobial peptide AL32-P113 with
527 enhanced antimicrobial activity *in vitro*. *Gene*. (in press).

528 Xia, Q. , Zhao , Q. F., Liao, Y., Zhu, W., Yu, G. H., Chen, F. Y., and Song, M. Y. (2013).
529 Optimization of conditions for the induction of antibacterial peptides and their crude extracts
530 activity in *Hermetia illucens*. *Chin J Environ Entomol*. 35, 44-48.

531 Yan, R., Liu, Y., Zhu, X. T., Yi, X. F., Liu, L., and Li, X. F. (2015). Effect of magnesium
532 cantharidate on hepatocellular carcinoma SMMC-7721 cells and subcutaneous hepatocellular
533 SMMC-7721 carcinoma transplantation tumors in nude mice. *Chin J Appl Entomo*l. 52,
534 477-485.

535 Yang, J., Xu, X., Hao, Y., Chen, J., Lu, H., Qin, J., Peng, L., and Chen, B. (2013). Expression
536 of DNA-PKcs and BRCA1 as prognostic indicators nasopharyngeal carcinoma following
537 intensity-modulated radiation therapy. *Oncol Lett*. 5, 1199-1204.

538 Zhang, L. (2015). Study on the Effect of Amphibian Antibacterial Peptide Temporin-1CEa
539 and Its Modified Peptides on Neovascularization and Metastasis of Melanoma. M. S. thesis,
540 Liaoning Normal University, Dalian.

541 **Figure captions**

542 **Figure 1** Separation crude extract from the hemolymph of *H. illucens* larvae by RP-HPLC

543 1) Separation of crude extract; 2) Purity detection of HI-3 by RP-HPLC

544

545 **Figure 2** MIC of HI-3 against four strains of bacteria

546

547 **Figure 3** Effects of HI-3 on proliferation inhibition rates of CNE2 Cells and HUV-C after 48

548 h treatment

549 Note: # means significant difference between the CNE2 cells group and HUV-C group under

550 the same concentration at the levels of 0.05. △ means this significant difference at the levels

551 of 0.01.

552

553 **Figure 4** Effects of HI-3 on morphology of CNE2 cells and HUV-C (400 ×)

554 Note: 1) CNE2 cells A: Negative control; B: 40 μg/ml; C: 80μg/ml; D: 160 μg/ml

555 2) HUV-C A: Negative control; B: 40 μg/ml; C: 80μg/ml; D: 160 μg/ml

556

557 **Figure 5** Apoptosis rates of CNE2 cells and HUV-C after treated with HI-3

558 Note: 1) CNE2 cells A: Negative control; B: 40 μg/ml; C: 80μg/ml; D: 160 μg/ml

559 2) HUV-C A: Negative control; B: 40 μg/ml; C: 80μg/ml; D: 160 μg/ml

560 3) Apoptosis rate of HUV-C and CNE2 cells after treated with HI-3 for 48 h. $^{\#}P < 0.05$

561 means the apoptosis of CNE2 cells were significantly higher when compared with

562 the CNE2 cells in the negative group. $^{\triangle}P < 0.05$ means there was significant

563 difference between CNE2 cells and HUV-C group.

564

565 **Figure 6** Effects of 160 μg/ml of HI-3 on the migration of CNE2 cells (100×)

566 1) Morphology observation, N: Negative control group; P: 160 μg/ml of HI-3 group

567 2) Migration rates of CNE2 cells

568

569 **Figure 7** Expression of telomerase hTERT and GAPDH in CNE2 cells after treated with HI-3

570 1) RT-PCR analysis on hTERT gene expression, Note: 1: Negative control group; 2: 160

571 μg/ml HI-3 group; 3: Standard nucleic acid molecule; 4, 5: Internal gene GAPDH;

572 2) Western blotting on hTERT protein expression;

573 **3)** Statistics of expression of hTERT protein.

574 **Table legends**

575 **Table 1** Inhibition zone diameters against the four strains of bacteria after treated with HI-1,

576 HI-2 and HI-3 (n=4, $\bar{x} \pm s$, mm)

577 Note: $^{\#}P < 0.05$ indicated there were significant differences in inhibition zone diameters

578 between HI-3 group and negative control. And $^{\triangle}P < 0.05$ indicated the inhibition zone

579 diameters in the *Bacillus subtilis* treatment were significantly lower when compared with the

580 *Staphylococcus aureus* and *Escherichia coli* treatments in the HI-3 group.

581

582 **Table 2** Effects of HI-1, HI-2 and HI-3 on proliferation inhibition rates of CNE2 cell (n=4,

583 $\bar{x} \pm s$, Inhibition rate：%)

584 Note: $^{\#}P < 0.05$ indicated that there were significant differences in the inhibition rates

585 between HI-3 group and HI-1/HI-2 group under the same concentration. $^{\triangle}P < 0.05$ indicated

586 that there were significant differences in inhibition rates between different time at the same

587 concentration of HI-3 group.

588

589 **Table 3** Effect of HI-3 on the expression of telomerase hTERT gene（n=6, $\bar{x} \pm s$ ）

590 Note: $^{\#}P < 0.05$ indicated that there were significant differences in expression levels between

591 HI-3 group and negative control group.

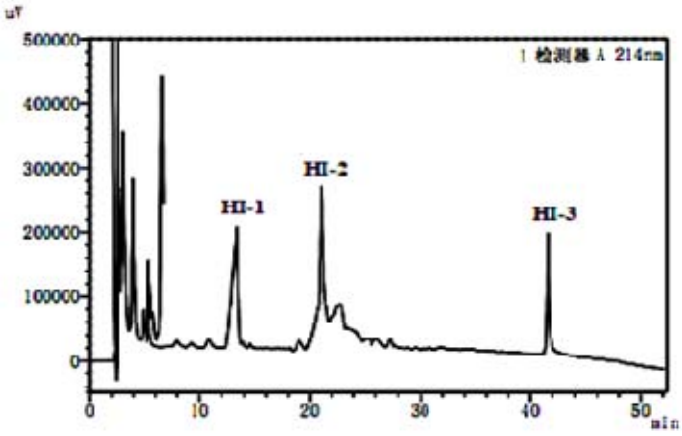

1)

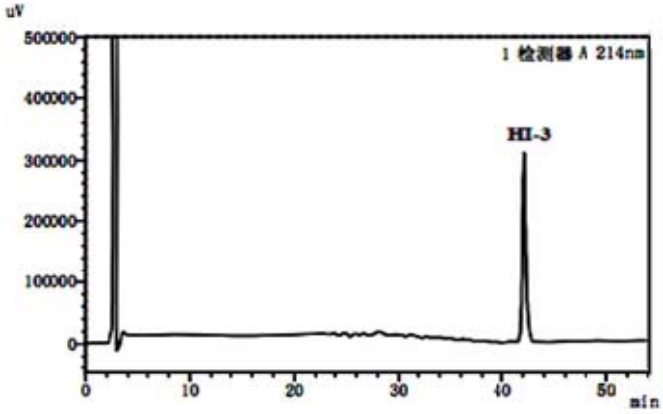

2)

Figure 1

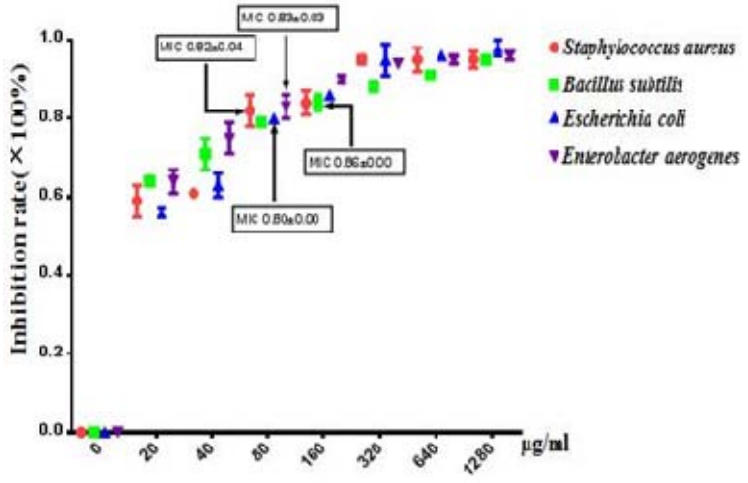

Figure 2

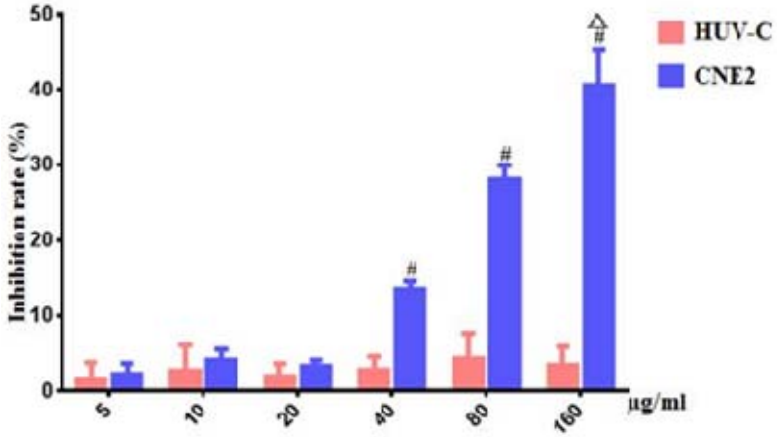

Figure 3

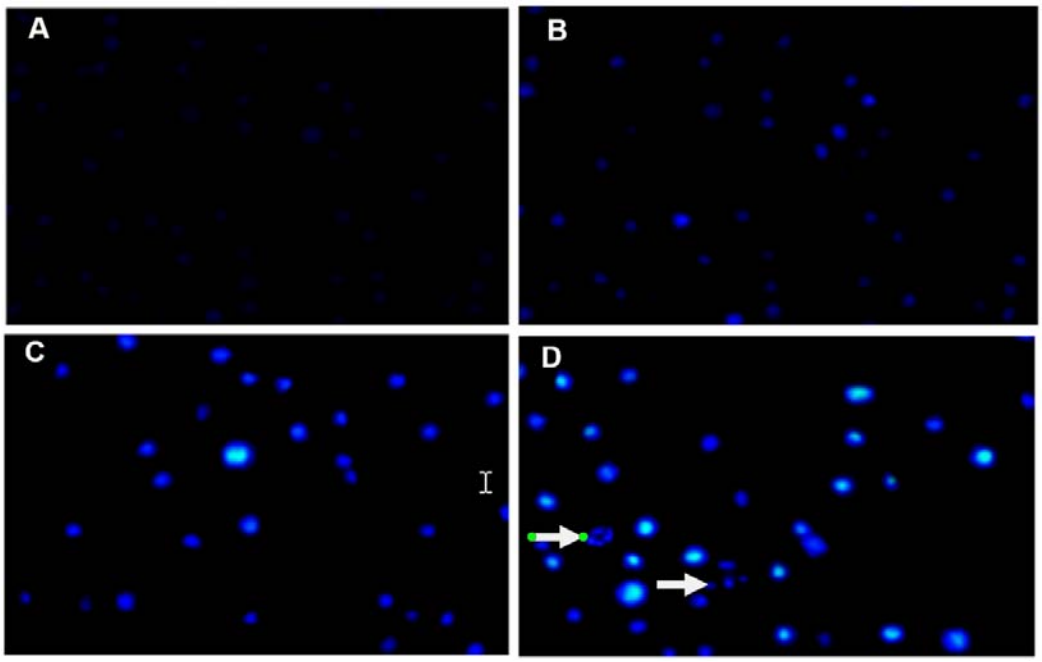

1)

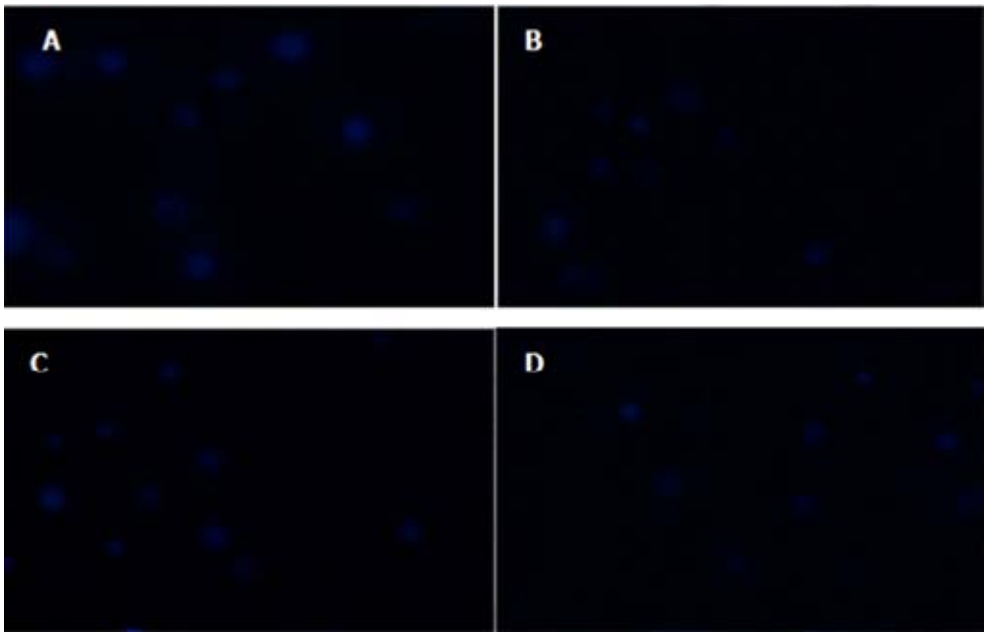

2)

Figure 4

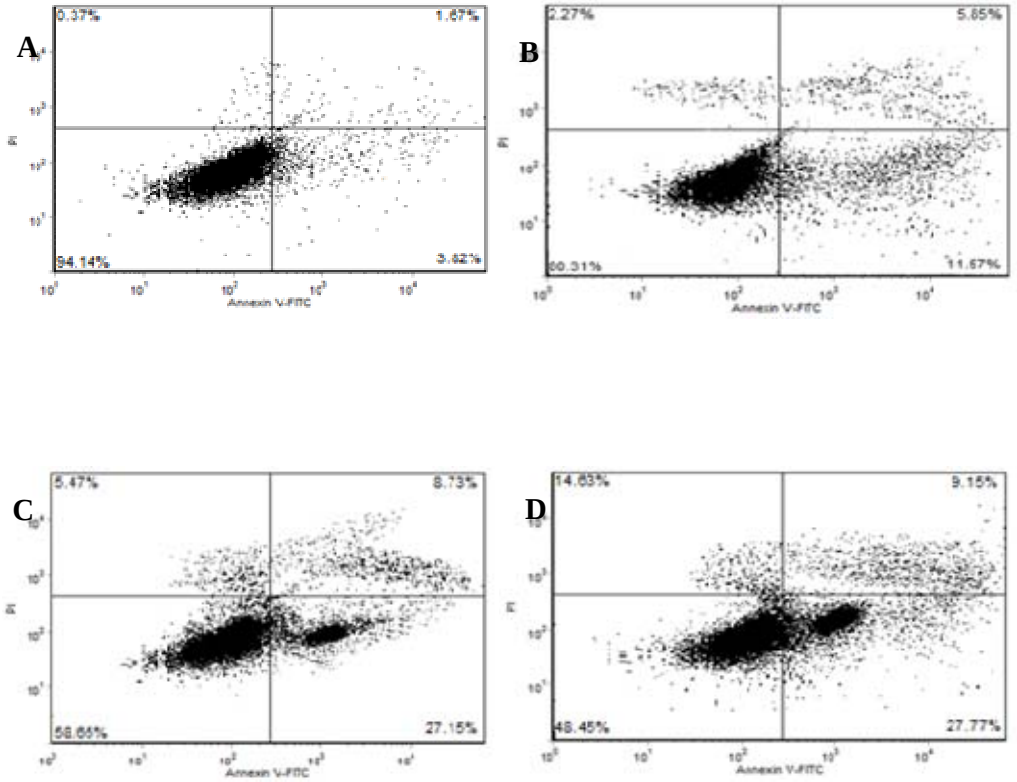

1)

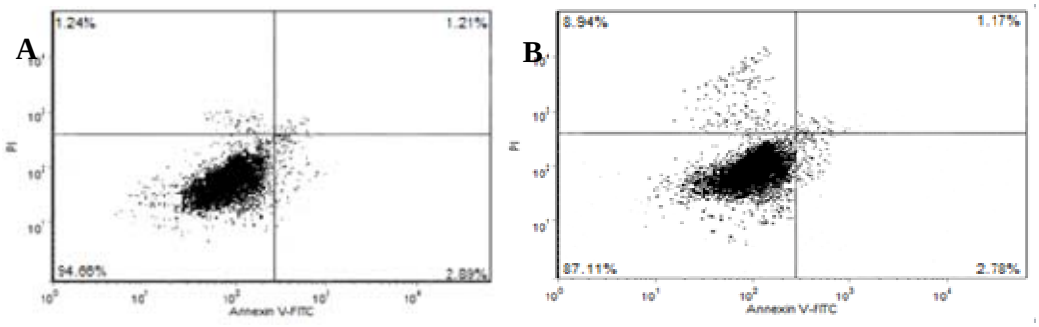

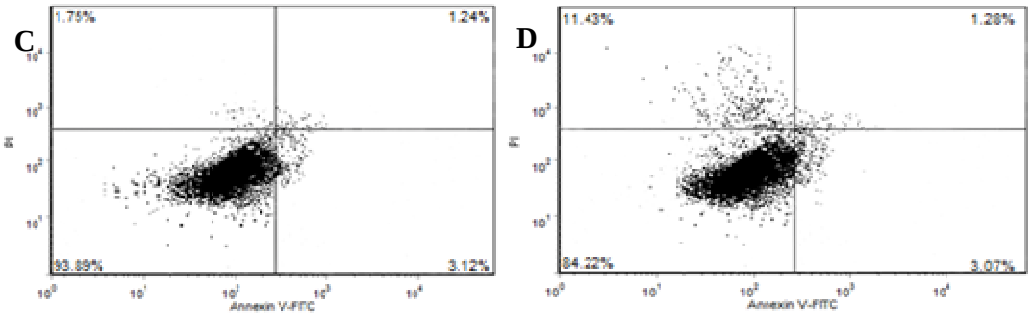

2)

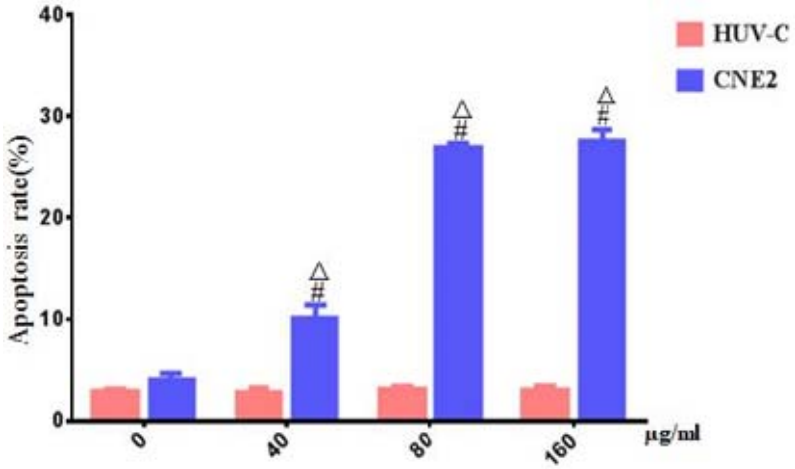

3)

Figure 5

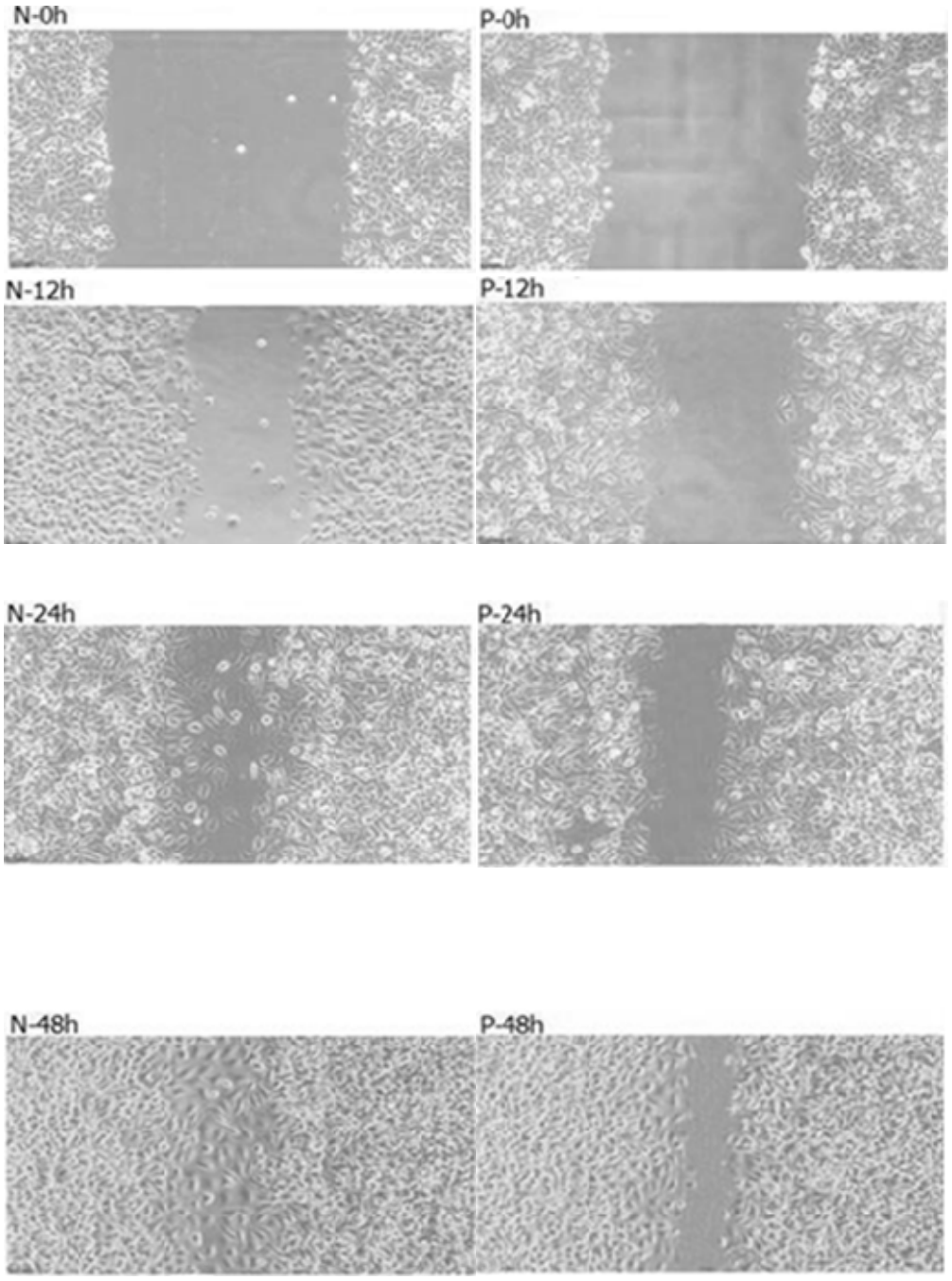

1)

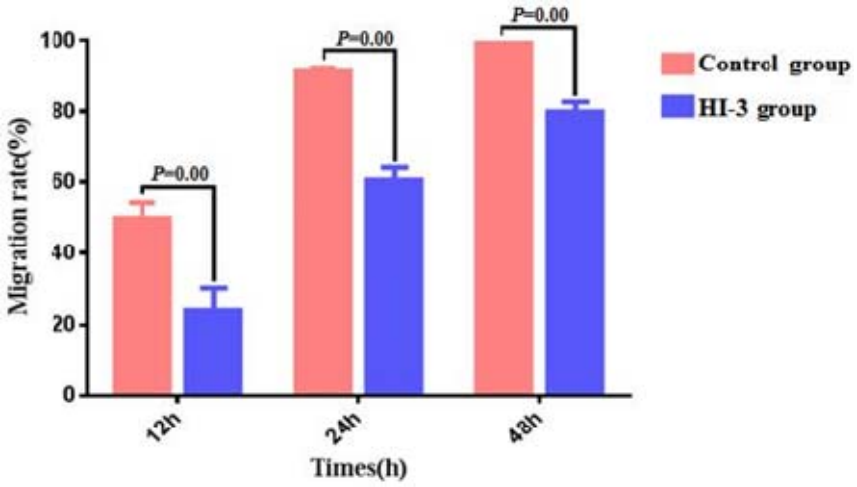

2)

Figure 6

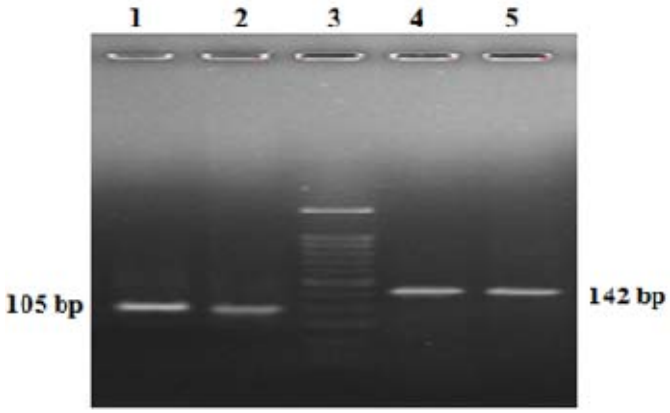

1)

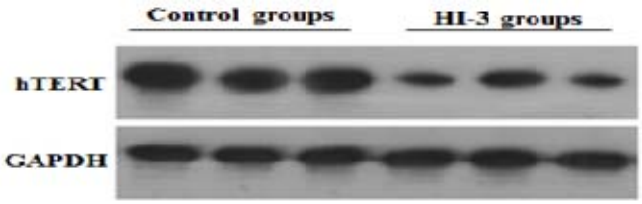

2)

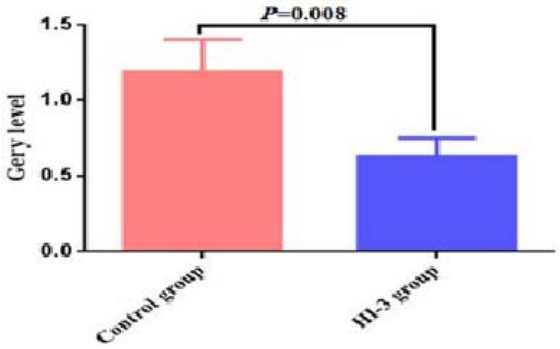

3)

Figure 7

Table 1

Groups	The bacterial strain			
	Staphylococcus aureus	*Bacillus subtilis*	*Escherichia coli*	*Enterobacter aerogenes*
Negative control	0.00±0.00	0.00±0.00	0.00±0.00	0.00±0.00
Gentamicin sulphate	18.99±0.50	15.71±0.68	17.64±0.51	16.27±0.75
HI-1	0.00±0.00	0.00±0.00	0.00±0.00	0.00±0.00
HI-2	0.00±0.00	0.00±0.00	0.00±0.00	0.00±0.00
HI-3	11.79±1.17$^{\#}$	10.84±1.00$^{\#\triangle}$	11.83±0.82$^{\#}$	11.41±0.78$^{\#}$

Table 2

Groups	Concentrations (μg/ml)	Times		
		12h	24h	48h
HI-1	5	2.98±0.20	1.43±0.43	1.96±0.35
	10	2.70±0.19	3.07±0.29	2.64±0.80
	20	2.44±0.13	2.60±0.37	2.57±0.13
	40	3.16±0.47	3.53±0.31	2.43±0.13
	80	3.37±0.33	3.90±0.34	4.38±0.33
	160	3.49±0.57	4.17±0.57	3.16±0.29
HI-2	5	1.78±0.24	1.08±0.7	2.15±0.61

	10	2.18±0.37	2.85±1.41	2.75±0.98
	20	2.93±0.78	2.48±0.29	2.29±0.06
	40	1.67±0.74	3.69±0.76	2.36±0.13
	80	3.25±0.14	3.87±0.56	4.16±0.14
	160	3.63±0.83	3.18±0.61	3.33±0.18
HI-3	5	2.18±0.94	1.83±0.76	2.28±1.42
	10	2.27±0.94	2.75±0.46	4.14±1.40
	20	1.74±0.04	4.07±1.58	3.33±0.77
	40	5.68±0.63 $^{\#}$	9.82±1.52$^{\#}$	13.49±1.06$^{\#}$
	80	10.94±1.43$^{\#}$	16.21±0.77$^{\#}$	28.09±1.84$^{\#}$
	160	17.80±1.02$^{\#}$	21.78±1.61$^{\#}$	40.56±6.80$^{\#\Delta}$

Table 3

Groups	hTERT Ct	GAPDH Ct	ΔCt	ΔΔCt	$2^{-\Delta\Delta Ct}$
HI-3	28.43±0.53	21.84±0.34	6.58±0.54$^{\#}$	1.51±0.54	0.37±0.15$^{\#}$
Negative control	25.56±0.26	20.48±0.20	5.07±0.41	0.00±0.41	1.03±0.31